13.7, 13.11t; 11.5

Received 1 February 1972

Acoustic Radiation from Two Spheroids

A. L. Van Buren and B. J. King

Naval Research Laboratory, Washington, D. C. 20390

The acoustic radiation from two spheroids whose surface normal velocity distributions are specified is calculated using a Green's function approach. To simplify the analysis only axially symmetrical problems are considered. The necessary Green's function is expanded in spheroidal wave functions about both spheroids. The unknown expansion coefficients are determined from the boundary condition that the normal derivative vanishes over both surfaces. An addition theorem which expresses spheroidal wave functions in one coordinate system in terms of spheroidal wave functions in another coordinate system was developed to facilitate application of this boundary condition. Numerical results for several different two-spheroid configurations and velocity distributions are presented and discussed. The straightforward extension to nonaxisymmetrical problems and to more than two spheroids is also discussed.

INTRODUCTION

The Helmholtz scalar wave equation is separable in both prolate and oblate spheroidal coordinates. Thus the acoustic radiation from spheroidal surfaces vibrating with a known normal velocity distribution can be calculated by use of eigenfunction expansions in terms of spheroidal wave functions. The large variety of shapes spanned by spheroidal geometry plus the recent development of FORTRAN computer programs[1-3] which accurately and rapidly evaluate spheroidal wave functions over a wide range of parameters has promoted a detailed investigation of spheroid radiation. However, previous studies have been restricted to single spheroids.[4-9]

This paper considers the acoustic radiation from two spheroids. The acoustic radiation is calculated using a Green's function technique similar to the one used by New[10] for the corresponding two-sphere problem. Here the Green's function is expanded in spheroidal wave functions about both spheroids. An addition theorem which expresses spheroidal wave functions in one coordinate system in terms of spheroidal wave functions in another coordinate system was developed[11] to facilitate application of homogeneous Neumann boundary conditions on the two spheroids in order to determine the unknown expansion coefficients. To simplify the analysis only axially symmetrical problems are considered. However, the results can be extended in a straightforward way to include more than two spheroids with arbitrary positions and orientations and arbitrary normal velocity distributions.

The analysis is presented in Sec. I. Numerical results for several different two-spheroid configurations and velocity distributions are presented and discussed in Sec. II. Configurations corresponding to a single spheroid near an infinite plane wall that is either rigid or soft are included. The conclusions are given in Sec. III.

I. ANALYSIS

The prolate spheroidal coordinates (ξ,η,ϕ) are related to Cartesian coordinates by the transformation

$$x=\frac{d}{2}(1-\eta^2)^{\frac{1}{2}}(\xi^2-1)^{\frac{1}{2}}\cos\phi,$$

$$y=\frac{d}{2}(1-\eta^2)^{\frac{1}{2}}(\xi^2-1)^{\frac{1}{2}}\sin\phi, \qquad (1)$$

$$z=\frac{d}{2}\xi\eta,$$

where d is the interfocal distance, and where $1\leq\xi<\infty$, $-1\leq\eta\leq 1$, and $0\leq\phi<2\pi$. This geometry is shown in Fig. 1. In the Cartesian coordinate system the surface of constant ξ is a prolate spheroid having a major axis of length ξd and a minor axis of length $(\xi^2-1)^{\frac{1}{2}}d$. The surface of constant η is one sheet of a hyperboloid of two sheets. The surface of constant ϕ is a half-plane, as in the spherical coordinate system.

The corresponding transformation for the oblate spheroidal coordinates is

$$x=\frac{d}{2}(1-\eta^2)^{\frac{1}{2}}(\xi^2+1)^{\frac{1}{2}}\cos\phi,$$
$$y=\frac{d}{2}(1-\eta^2)^{\frac{1}{2}}(\xi^2+1)^{\frac{1}{2}}\sin\phi, \qquad (2)$$
$$z=\frac{d}{2}\xi\eta,$$

where now $0\leq\xi<\infty$, $-1\leq\eta\leq 1$, and $0\leq\phi<2\pi$.

The oblate geometry is shown in Fig. 2. Here the surface of constant ξ is an oblate spheroid having a major axis of length $(\xi^2+1)^{\frac{1}{2}}d$ and a minor axis of length ξd. The surface of constant η is a hyperboloid of one sheet. The oblate spheroidal coordinate system can be obtained from the prolate spheroidal coordinate system by use of the interchange $\xi\rightarrow i\xi$ and $d\rightarrow -id$. Expressions developed for prolate spheroidal geometry can be converted into analogous expressions for oblate spheroidal geometry by use of the same interchange. Consequently, although only the prolate expressions are given explicitly in the following discussion, the corresponding oblate expressions are also valid.

Consider two spheroidal surfaces S_1 and S_2, which are parallel and share a common z axis, as shown in Fig. 3. Spheroidal coordinate systems $C_1(\xi_1,\eta_1,\phi_1)$ and $C_2(\xi_2,\eta_2,\phi_2)$ are established which contain S_1 ($\xi_1=\xi_{10}$) and S_2 ($\xi_2=\xi_{20}$), respectively, as natural coordinate surfaces. The interfocal lengths of the two systems are d_1 and d_2, and the separation of their origins is r_{12}. The region outside both S_1 and S_2 is assumed to be filled with an infinite homogeneous fluid of mass density ρ and sound speed c. The surfaces S_1 and S_2 are assumed to be vibrating with rotationally symmetrical normal

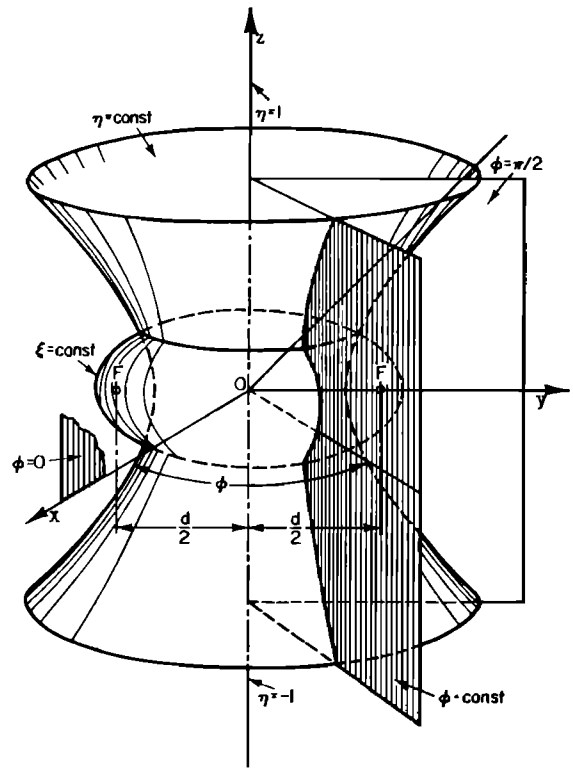

FIG. 2. The oblate spheroidal coordinate system.

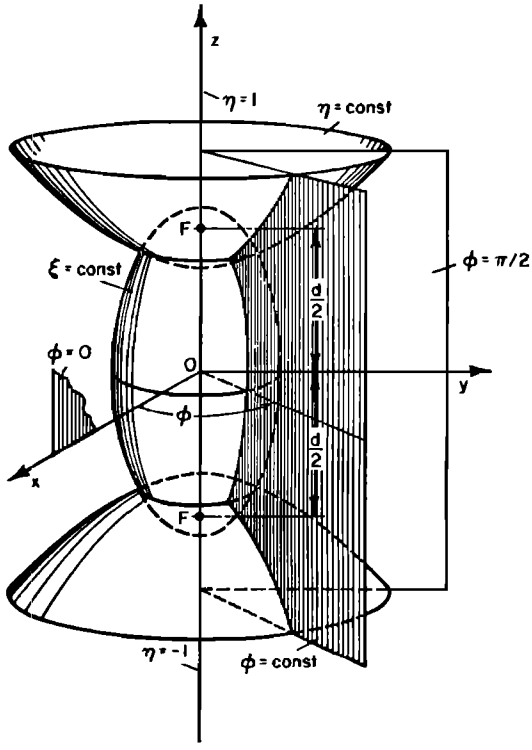

FIG. 1. The prolate spheroidal coordinate system.

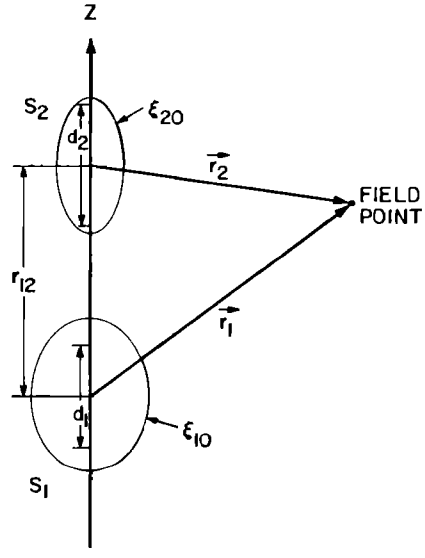

FIG. 3. The two-spheroid geometry.

velocity distributions whose spatial dependences are given by $v_1(\eta_1)$ and $v_2(\eta_2)$. The time dependence is taken to be harmonic, with the factor $e^{i\omega t}$ being suppressed.

The acoustic pressure produced at a point $\mathbf{r}$ exterior to both S_1 and S_2 can be obtained by use of the integral formulation[12]

$$p(\mathbf{r})=\frac{i\omega\rho}{4\pi}\left[\int_{S_1} v_1(\eta_1')G(\mathbf{r},\mathbf{r}')dS(\mathbf{r}') + \int_{S_2} v_2(\eta_2')G(\mathbf{r},\mathbf{r}')dS(\mathbf{r}')\right], \quad (3)$$

where the Green's function $G(\mathbf{r},\mathbf{r}')$ is the solution to the equation

$$[\nabla^2(\mathbf{r}')+k^2]G(\mathbf{r},\mathbf{r}')=-4\pi\delta(\mathbf{r}'-\mathbf{r}) \quad (4)$$

which satisfies the radiation condition at infinity and whose outward normal derivative $\partial G(\mathbf{r},\mathbf{r}')/\partial n$ vanishes over both S_1 and S_2. Here $k=2\pi/\lambda$, where λ is the wavelength. The Green's function is obtained by a procedure analogous to that used by New[10] for the two-sphere problem.

First the Green's function is written as a sum of the free-space Green's function, which is the particular solution to Eq. 4, and scattering contributions from both S_1 and S_2, which form the complementary solution and are expressed as eigenfunctions of the homogeneous equation $(\nabla^2+k^2)\Psi=0$. The extension to more than two spheroids would require the addition of scattering contributions to include every spheroid. Since the normal velocity distribution is chosen to be rotationally symmetrical, only the $m=0$ terms in the Green's function contribute to the resulting rotationally symmetrical acoustic pressure. To simplify the analysis, the $m\neq 0$ terms will be dropped, but the analysis could be extended for an arbitrary normal velocity distribution. Thus, the effective Green's function is given by

$$G_0(\mathbf{r},\mathbf{r}')=\left[\frac{e^{-ik|\mathbf{r}-\mathbf{r}'|}}{|\mathbf{r}-\mathbf{r}'|}\right]_{m=0}+\sum_{l=0}^{\infty} A_l\Psi_{0l}^{(4)}(h_1;\xi_1',\eta_1') + \sum_{l=0}^{\infty} B_l\Psi_{0l}^{(4)}(h_2;\xi_2',\eta_2'), \quad (5)$$

where the spheroidal wave functions for $m=0$ are given by

$$\Psi_{0l}^{(4)}(h;\xi,\eta)=R_{0l}^{(1)}(h,\xi)S_{0l}^{(1)}(h,\eta) - iR_{0l}^{(2)}(h,\xi)S_{0l}^{(1)}(h,\eta) = \Psi_{0l}^{(1)}(h;\xi,\eta)-i\Psi_{0l}^{(2)}(h;\xi,\eta). \quad (6)$$

Here (ξ_1',η_1',ϕ_1') and (ξ_2',η_2',ϕ_2') are the spheroidal coordinates of $\mathbf{r}'$ in C_1 and C_2, and the acoustic size parameters $h_1=kd_1/2$ and $h_2=kd_2/2$. The spheroidal angle wave function of the first kind $S_{0l}^{(1)}(h,\eta)$ and the spheroidal radial wave functions of the first and second kind $R_{0l}^{(1)}(h,\xi)$ and $R_{0l}^{(2)}(h,\xi)$ used in this report are defined by Flammer.[13] The angle function can be expanded in a series in the corresponding Legendre functions

$$S_{0l}^{(1)}(h,\eta)=\sum_{n=0,1}^{\infty}{}' d_n(h|0l)P_n(\eta), \quad (7)$$

where the prime indicates that the summation is over even or odd values of n according to whether l is even or odd. The radial functions $R_{0l}^{(1)}(h,\xi)$ and $R_{0l}^{(2)}(h,\xi)$ correspond to spherical Bessel functions of the first and second kinds and are normalized so that $\Psi_{0l}^{(4)}(h;\xi,\eta)$ represents outgoing waves for $e^{i\omega t}$ time dependence.

The free space Green's function can be expanded in terms of spheroidal wave functions in either C_1 or C_2. The $m=0$ term is given by

$$\left[\frac{e^{-ik|\mathbf{r}-\mathbf{r}'|}}{|\mathbf{r}-\mathbf{r}'|}\right]_{m=0} = \sum_{l=0}^{\infty}\left(\frac{-2ik}{N_{0l}}\right)\begin{cases}\Psi_{0l}^{(1)}(h;\xi,\eta)\Psi_{0l}^{(4)}(h;\xi',\eta'), & \xi<\xi',\\ \Psi_{0l}^{(4)}(h;\xi,\eta)\Psi_{0l}^{(1)}(h;\xi',\eta'), & \xi>\xi',\end{cases} \quad (8)$$

where

$$N_{0l}=\int_{-1}^{1}[S_{0l}^{(1)}(h,\eta)]^2d\eta=\sum_{n=0,1}^{\infty}{}'\frac{2d_n^2(h|0l)}{(2n+1)}. \quad (9)$$

The effective Green's function which results from combining Eqs. 5 and 8 contains spheroidal wave functions in both coordinate systems C_1 and C_2. Application of the boundary conditions on S_1 or S_2 in order to determine A_l and B_l is difficult if $G_0(\mathbf{r},\mathbf{r}')$ is not expressed entirely in C_1 or C_2, respectively. Fortunately, this can be accomplished by the use of a spheroidal addition theorem which expresses a spheroidal wave function with reference to one coordinate frame in terms of spheroidal wave functions with reference to a second coordinate frame. The general addition theorem for spheroidal wave functions which is derived in Ref. 11 allows for arbitrary relative position and orientation of the two coordinate frames and is applicable whether the two spheroidal coordinate frames are both prolate, both oblate, or one prolate and one oblate. For the present application, the addition theorem reduces to the following form:

$$\Psi_{0l}^{(4)}(h_i;\xi_i',\eta_i')=\sum_{n=0}^{\infty}C_{ln}^{ij}\Psi_{0n}^{(1)}(h_j;\xi_j',\eta_j'), \quad (10)$$

where

$$C_{ln}^{ij}=\sum_{r=0,1}^{\infty}{}' i^{r-l}d_r(h_i|0l) \times\sum_{s=0,1}^{\infty}{}'\left(\frac{2}{2s+1}\right)\sum_{t=|r-s|}^{r+s}{}' a(s,t,r,0,0) \times h_t^{(2)}(kr_{12})P_t(\cos\theta_{ji})i^{s-n}d_s(h_j|0n)/N_{0n}, \quad (11)$$

with the prime sign indicating that the summation is in steps of two, and that s or r is taken to be even or odd according to whether n or l is even or odd. The function $h_l^{(2)}(kr_{12})$ is a spherical Hankel function of the second kind. The angles θ_{21} and θ_{12} are equal to 0 and π, respectively, so that $P_l(\cos\theta_{21})=1$ and $P_l(\cos\theta_{12})=(-1)^l$. The coefficient $a(s,t,r,0,0)$ is given by

$$a(s,t,r,0,0) = \frac{(-1)^\lambda(2s+1)(2t+1)(2\lambda)!(2\lambda_1)!(2\lambda_2)!(\Lambda!)^2}{(2\Lambda+1)!(\lambda!\lambda_1!\lambda_2!)^2}, \quad (12)$$

where $\Lambda=(r+s+t)/2$, $\lambda=\Lambda-r$, $\lambda_1=\Lambda-s$, $\lambda_2=\Lambda-t$.

Use of the addition theoremf or $i=2$ and $j=1$ leads to the following form of the effective Green's function expressed entirely in C_1:

$$G_0(\mathbf{r},\mathbf{r}') = \sum_{l=0}^{\infty}\left(\frac{-2ik}{N_{0l}}\right)\Psi_{0l}^{(4)}(h_1;\,\xi_1,\eta_1)\Psi_{0l}^{(1)}(h_1;\,\xi_1',\eta_1') + \sum_{l=0}^{\infty}\Big[A_l\Psi_{0l}^{(4)}(h_1;\,\xi_1',\eta_1') + B_l\sum_{n=0}^{\infty}C_{ln}{}^{21}\Psi_{0n}^{(1)}(h_1;\,\xi_1',\eta_1')\Big], \quad (13)$$

where $\xi_1>\xi_1'$, as required for the present discussion.

Differentiating $G_0(\mathbf{r},\mathbf{r}')$ with respect to ξ_1', setting this equal to zero at $\xi_1'=\xi_{10}$, multiplying by $S_{0q}^{(1)}(h_1,\eta_1')d\eta_1'$, and integrating over η_1' from -1 to 1, the range of orthogonality for the spheroidal angle wave functions, one obtains the following set of equations:

$$\dot{R}_{0q}^{(4)}(h_1,\xi_{10})A_q+\dot{R}_{0q}^{(1)}(h_1,\xi_{10})\sum_{l=0}^{\infty}C_{lq}{}^{21}B_l = \left(\frac{2ik}{N_{0q}}\right)\dot{R}_{0q}^{(1)}(h_1,\xi_{10})\Psi_{0q}^{(4)}(h_1;\,\xi_1,\eta_1),\quad q=0\text{ to }\infty, \quad (14)$$

where the dot indicates the derivative with respect to ξ. The effective Green's function can also be expressed entirely in C_2 in order to apply the boundary condition on S_2. Use of the procedure indicated above leads to the additional set of equations:

$$\dot{R}_{0q}^{(4)}(h_2,\xi_{20})B_q+\dot{R}_{0q}^{(1)}(h_2,\xi_{20})\sum_{l=0}^{\infty}C_{lq}{}^{12}A_l = \left(\frac{2ik}{N_{0q}}\right)\dot{R}_{0q}^{(1)}(h_2,\xi_{20})\Psi_{0q}^{(4)}(h_2;\,\xi_2,\eta_2),\quad q=0\text{ to }\infty. \quad (15)$$

In theory, the doubly infinite set of simultaneous equations obtained by combining Eqs. 14 and 15 can be solved for the unknowns A_l and B_l, $l=0$ to ∞. In practice, the summations over l in Eq. 13 are truncated at $l=L$ and the resulting $2L+2$ equations are solved for A_l and B_l, $l=0$ to L. The choice for L depends on the normal velocity distributions $v_1(\eta_1')$ and $v_2(\eta_2')$ and the required accuracy of the results. An estimate for L is given by the highest order that must be retained in the expansion of $v_1(\eta_1')$ and $v_2(\eta_2')$ in terms of the appropriate spheroidal angle wave functions in order to represent them to within the required accuracy. Equations 14 and 15 can be written in the following truncated form:

$$\sum_{l=0}^{2L+1}M_{ql}b_l\doteq g_q,\quad q=0\text{ to }2L+1, \quad (16)$$

where the elements M_{ql} form a square matrix and depend only on the frequency and the geometry of the two spheroids, the elements $b_l=A_l$ for $l=0$ to L and $b_l=B_{l-L-1}$ for $l=L+1$ to $2L+1$, and the right-hand side elements g_q are the functions $\Psi_{0q}^{(4)}(h_1;\,\xi_1,\eta_1)$ for $q=0$ to L and $\Psi_{0,q-L-1}^{(4)}(h_2;\,\xi_2,\eta_2)$ for $q=L+1$ to $2L+1$. The symbol $\doteq$ indicates that L is chosen large enough to ensure the desired accuracy in the final results. Note that A_l and B_l depend on the field point only through the right-hand side. Equation 16 can be inverted to give

$$b_l\doteq\sum_{q=0}^{2L+1}M_{lq}{}^{-1}g_q, \quad (17)$$

so that once the inverse elements have been obtained for a given frequency and geometry, A_l and B_l and, consequently, the effective Green's function can be calculated for any field point by simple matrix multiplication.

The acoustic pressure is now evaluated from Eq. 3. Consider the first term, where the area element is given by

$$dS=(d_1^2/4)(\xi_{10}^2-1)^{\frac{1}{2}}(\xi_{10}^2-\eta_1'^2)^{\frac{1}{2}}d\eta_1'd\phi_1'. \quad (18)$$

Expressing the $\mathbf{r}'$ dependence of the effective Green's function entirely in C_1 and integrating, one obtains

$$p_1(\mathbf{r})\doteq\sum_{l=0}^{L}D_{l+L+1}\Psi_{0l}^{(4)}(h_2;\,\xi_2,\eta_2) + \sum_{l=0}^{L}E_l\Psi_{0l}^{(4)}(h_1;\,\xi_1,\eta_1), \quad (19)$$

where

$$D_l=[ih_1^2\rho c(\xi_{10}^2-1)^{\frac{1}{2}}/2k]\sum_{q=0}^{L}\Big[M_{ql}{}^{-1}R_{0q}^{(4)}(h_1,\xi_{10})I_{0q} + M_{q+L+1,l}{}^{-1}\sum_{n=0}^{\infty}C_{qn}{}^{21}R_{0n}^{(1)}(h_1,\xi_{10})I_{0n}\Big], \quad (20)$$

and

$$E_l=D_l+h_1^2\rho c(\xi_{10}^2-1)^{\frac{1}{2}}R_{0l}^{(1)}(h_1,\xi_{10})I_{0l}/N_{0l}, \quad (21)$$

with

$$I_{0l}=\int_{-1}^{1}(\xi_{10}^2-\eta_1'^2)^{\frac{1}{2}}v_1(\eta_1')S_{0l}^{(1)}(h_1,\eta_1')d\eta_1'. \quad (22)$$

These expressions give the acoustic pressure when S_1

is vibrating and $v_2(\eta_2')$ is identically zero, so that S_2 acts only as a rigid scatterer. When S_2 is vibrating also, the second term in Eq. 3 must be included. The corresponding expressions for this contribution to the acoustic pressure can be obtained from Eqs. 19–22 by the simple interchange of subscripts 1 and 2. In order to simplify the resulting mathematical expressions the remainder of the analysis will be restricted to the case where only S_1 vibrates, i.e., where the total acoustic pressure is given by $p_1(\mathbf{r})$.

The acoustic pressure in the farfield is obtained from Eq. 19 with the use of the limiting form for the spheroidal wave functions. This gives

$$p_{FF}(r_1,\theta_1)\doteq\frac{e^{-ikr_1}}{r_1}f(\theta_1), \tag{23}$$

where

$$f(\theta_1)=\sum_{l=0}^{L} i^{l+1}[D_{l+L+1}\exp(ikr_{12}\cos\theta_1)S_{0l}^{(1)}(h_2,\cos\theta_1) +E_lS_{0l}^{(1)}(h_1,\cos\theta_1)], \tag{24}$$

and where (r_1,θ_1,ϕ_1) are the spherical coordinates of the farfield point relative to S_1. The function $|f(\theta_1)|$ is called the farfield pressure distribution.

In the following discussion the region of the spheroidal surface S_1 bounded by the curves $\eta=\eta_{1L}$ and $\eta=\eta_{1U}$ is assumed to vibrate with uniform normal velocity V_1, while the remainder of S_1 is assumed to be rigid. For the case of uniform vibration, the normalized self-acoustic radiation impedance z is defined by

$$z=r+ix=\left(\frac{1}{\rho cV_1S}\right)\int_{\eta_{1L}}^{\eta_{1U}} p(\eta_1)dS(\mathbf{r}), \tag{25}$$

where the real quantities r and x are the normalized self-acoustic radiation resistance and the normalized self-acoustic radiation reactance, respectively, and where S is the area of the vibrating region. The less descriptive names radiation impedance, radiation resistance, and radiation reactance will be used in the remainder of the paper. Note that the use of Eq. 25 requires a knowledge of the acoustic pressure over the surface S_1. Although the free-space Green's function and, consequently, the effective Green's function is singular at the point $\mathbf{r}=\mathbf{r}'$ so that the expansions given in Eq. 8 do not converge at that point, the singularity is integrable, and the resulting expression for the acoustic pressure given in Eq. 19 converges to the correct value for field points on S_1. Expressing $p_1(\mathbf{r})$ entirely in C_1 by use of the addition theorem given in Eq. 10 and integrating, one obtains

$$z\doteq\frac{d_1^2\pi(\xi_{10}^2-1)^{\frac{1}{2}}}{2\rho cV_1S}\sum_{l=0}^{L}[E_lR_{0l}^{(4)}(h_1,\xi_{10})I_{0l} +D_{l+L+1}\sum_{n=0}^{\infty} C_{ln}^{21}R_{0n}^{(1)}(h_1,\xi_{10})I_{0n}]. \tag{26}$$

II. NUMERICAL RESULTS AND DISCUSSION

The calculation of the acoustic radiation from two spheroids by use of the expressions derived in Sec. I requires numerical values for the spheroidal angle and radial wave functions and for the integrals I_{0l} given in Eq. 22 with $v(\eta)=V$ for $\eta_L\leq\eta\leq\eta_U$, and $v(\eta)=0$ elsewhere. Accurate values for the spheroidal wave functions were obtained using PRAD,[1] OBRAD,[2] and ANGLFN,[3] FORTRAN computer programs written in double precision arithmetic for the CDC 3800 computer at the Naval Research Laboratory. These computer programs were developed recently to evaluate spheroidal wave functions with greater accuracy over a wider range of parameters than previously available. Extensive tables[14,15] of both prolate and oblate spheroidal radial wave functions obtained using PRAD and OBRAD have recently been published. These tables contain entries for values of $m=0, 1, 2$; $l=m(1)m+49$ for a wide range of values of ξ and h. The integrals I_{0l} were evaluated by a procedure involving expansion of the spheroidal angle wave functions in a series of Legendre polynomials, as shown in Eq. 7, subsequent expansion of the Legendre polynomials in a series in terms of $\cos r\theta$ where $\theta=\cos^{-1}\eta$, and computation of the resulting integrals

$$J_r=\int_{\eta_L}^{\eta_U}(\xi_0^2-\eta^2)^{\frac{1}{2}}\cos r\theta d\eta, \quad r=0, 1, \cdots, \tag{27}$$

by use of Gaussian quadrature.

In the first example, consider two disks with $ka=1.0$, where a is the radius, which are parallel, coaxial, and separated by a distance $r_{12}=2a$ so that $kr_{12}=2.0$. Note that the disk is a limiting shape for the oblate spheroid and corresponds to the shape parameter $\xi=0$. The acoustic size parameter h is equal to 1.0, since h and ka

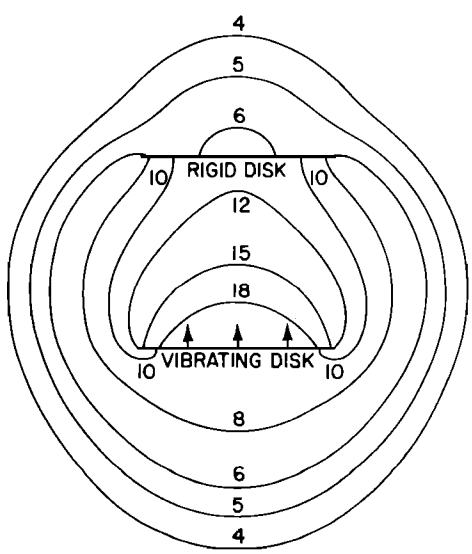

FIG. 4. The nearfield pressure distribution in decibels for a disk vibrating in the presence of a rigid disk.

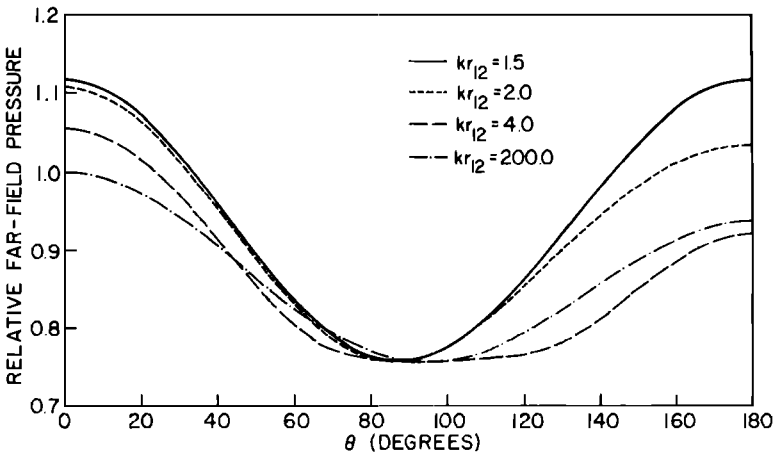

FIG. 5. The farfield pressure distribution for a disk vibrating in the presence of a rigid disk.

are equivalent for a disk. The top surface of the lower disk is vibrating uniformly with a velocity amplitude of 1.0 m/sec. The bottom surface of the lower disk and the entire upper disk are rigid. The acoustic pressure field in the vicinity of the disks is shown in Fig. 4. The lines represent isobars and connect points of equal pressure amplitude. The numbers labeling the isobars have the units of decibels relative to a pressure of 1 bar. Note that the isobars approach the rigid surfaces at right angles. If this were not true, the normal gradient of the pressure at the surface would be nonzero and would produce a nonzero normal component of the particle velocity, in contradiction with the assumed boundary condition. The moderately large pressure that exists in the so-called shadow region immediately behind the rigid disk is not surprising since ka is not very large.

The farfield pressure distribution for this two-disk configuration is given by the curve labeled $kr_{12}=2.0$ in Fig. 5. The polar angle θ is measured in the customary way so that the center of the rigid disk is in the direction of zero degrees (called the forward direction). Figure 5 also shows the farfield pressure distribution for the two disks when the separation is such that $kr_{12}=1.5$, 4.0, or 200.0. Results obtained for values of kr_{12} greater than 200.0 are indistinguishable from those for $kr_{12}=200.0$, indicating that the effect of the rigid disk is negligible for these large separations. Thus the curve for $kr_{12}=200.0$ is also the farfield pressure distribution for the vibrating disk alone. The farfield pressure distributions are normalized so that the value in the forward direction is equal to unity for this free-field case. As expected, the effect of the rigid disk is greater when the two disks are closer together. When $kr_{12}=1.5$ or 2.0, the farfield radiation is increased in both the forward and backward directions but remains virtually unchanged in the lateral direction. For $kr_{12}=4.0$, phase

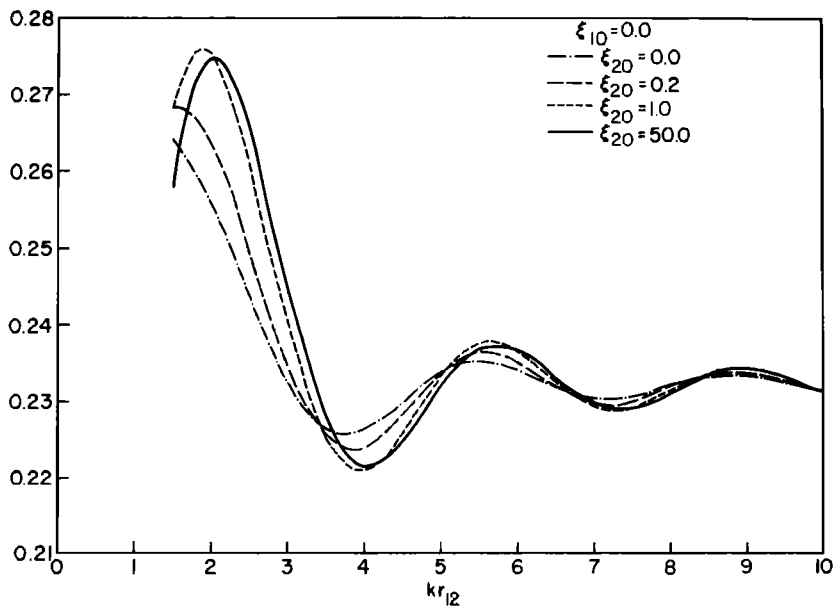

FIG. 6. The normalized radiation resistance as a function of the distance of separation kr_{12} for a disk vibrating in the presence of a rigid oblate spheroid.

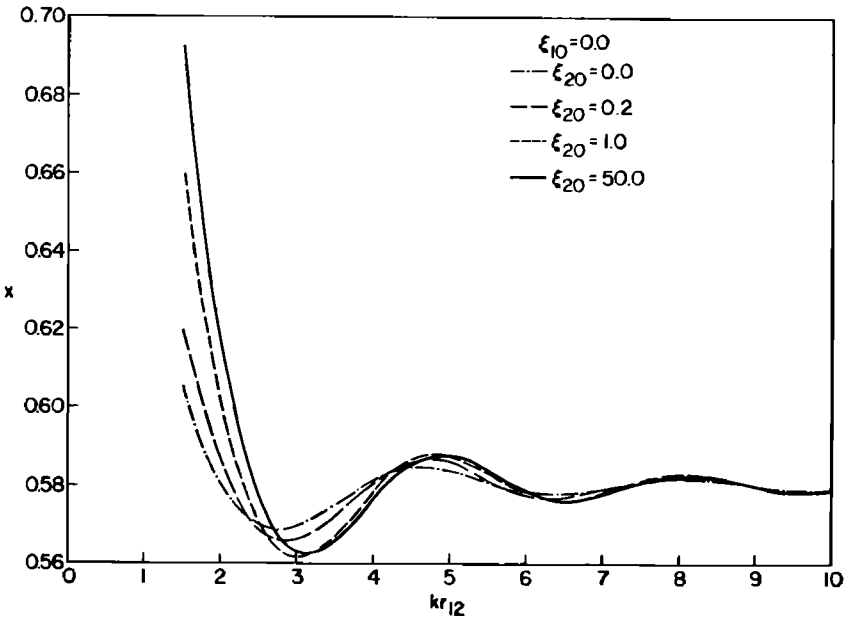

FIG. 7. The normalized radiation reactance as a function of the distance of separation kr_{12} for a disk vibrating in the presence of a rigid oblate spheroid.

cancellation decreases the backward radiation although the radiation is increased in the forward direction.

The effect that the rigid disk has on the radiation impedance of the source is indicated in Figs. 6 and 7. Here the radiation resistance r and the radiation reactance x are plotted as a function of the separation of the disks kr_{12} for $1.5 \leq kr_{12} < 10.0$. Because of slow convergence in the calculation of the transformation coefficient C_{ln}^{ij} for small values of kr_{12}, economical computation of the radiation impedance for $kr_{12} < 1.5$ would require more core storage than was available in the computer used for these calculations. The curves for $\xi_{20}=0$ correspond to the two-disk configuration described above. The other curves give the radiation impedance when the rigid disk is replaced by a rigid oblate spheroid with a shape parameter $\xi_{20}=0.2$, 1.0, or 50.0. These shape parameters correspond to major to minor axis ratios of 5.0990, 1.4142, and 1.0002, so that the spheroids can be described as moderately thin, moderately fat, and nearly spherical, respectively. Values for the acoustic size parameter h_2 were chosen so that the semimajor axis of each rigid oblate spheroid $h_2(\xi_{20}^2+1)^{\frac{1}{2}}/k$ is equal to the radius of the source $1.0/k$.

The periodic variations in both the radiation resistance and the radiation reactance are produced by interference with the radiation scattered from the rigid oblate spheroid. The effect of this scattering decreases rapidly with increasing kr_{12} so that the impedance at $kr_{12}=10.0$ is nearly equal to that of the vibrating disk alone. The primary effect produced by changing the shape of the rigid oblate spheroid while keeping its projected area constant is to move the effective scattering center. Since most of the radiation scattered back onto the source comes from the half of the rigid oblate spheroid that is facing the source, the effective separation between the two spheroids is less than kr_{12} unless $\xi_{20}=0$. Thus the interference maxima and minima are shifted toward larger values of kr_{12}, the maximum displacement occurring for $\xi_{20}=50.0$.

An important class of radiation problems that can be solved using two-spheroid geometry concerns the radiation of a single spheroid in the presence of an infinite plane wall that is either rigid or soft (zero acoustic pressure). The solution for the rigid-wall case can be obtained by replacing the wall by an image spheroid vibrating in phase with the original spheroid and then solving the resulting two-spheroid problem. Similarly, the soft or pressure release wall is replaced by an image spheroid vibrating 180° out of phase with the original spheroid.

As an example, consider a disk with $ka=1.0$, vibrating uniformly on both sides and situated parallel to and a distance s from an infinite plane wall. Solution of the corresponding two-disk problems leads to the radiation resistance and reactance for both a rigid and a soft wall, as plotted vs ks in Figs. 8 and 9. The interlacing of the curves is related to the fact that a plane wave which is reflected at a nongrazing angle from an infinite plane wall undergoes a phase shift of 0° when the wall is rigid and 180° when it is soft. The values of the radiation resistance and reactance at the crossing points are in good agreement with the radiation impedance of the vibrating disk when no wall is present, $z_0=0.423+0.647i$.

If the vibrating disk were very small acoustically, monopole theory could be used to calculate the contribution of the wall to the radiation impedance. The only effect of the wall to be considered when using monopole theory is that due to radiation which is scattered once from the wall back onto the source. Multiple scattering is not considered. In the corresponding two-disk problem, the single scattering from the wall is replaced by the direct radiation from the image disk. Straight-

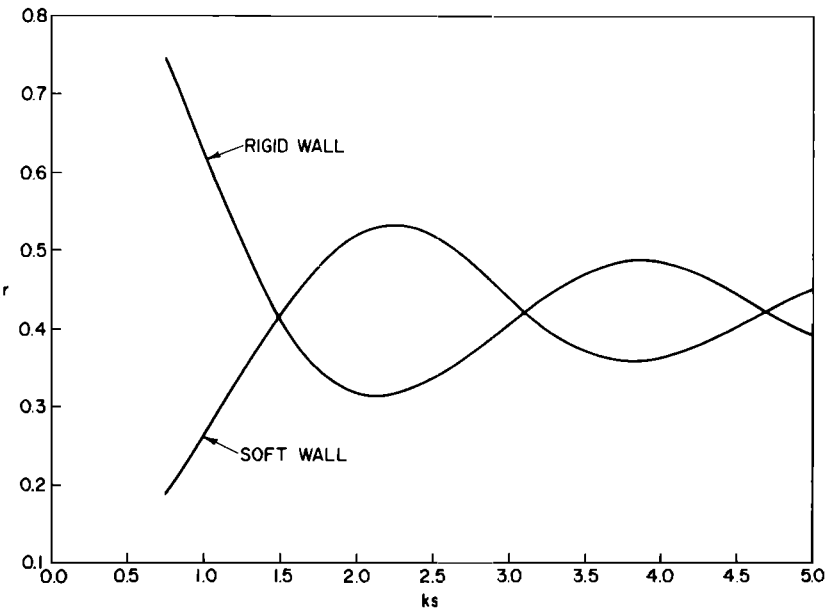

FIG. 8. The normalized radiation resistance as a function of the distance of separation ks for a disk vibrating in the presence of an infinite plane wall that is either rigid or soft.

forward calculation using monopole theory yields

$$z=z_0+\Delta z$$
$$=z_0\pm 0.5i(ka)^2h_0^{(2)}(2ks), \qquad (28)$$

where $h_0^{(2)}(2ks)$ is the spherical Hankel function of the second kind, and where the + or − sign is used when the wall is rigid or soft, respectively. Although the monopole approximation is not strictly valid for the present case where $ka=1.0$, it does qualitatively describe the behavior of the curves. As expected, the agreement improves as ks increases and the contribution from multiple scattering decreases.

As a final example, consider a prolate spheroid whose entire surface is vibrating uniformly. Its shape parameter ξ is equal to 1.1, corresponding to a major to minor axis ratio of 2.4004. The acoustic size parameter h is chosen equal to 2.1822 so that k times the semiminor axis is equal to unity. The farfield pressure distribution as a function of the polar angle θ is given by the solid curve in Fig. 10. Because of even symmetry about $\theta=90°$, the broadside direction, only half of the distribution is shown. The other two curves in this figure show the farfield pressure distribution when an infinite plane wall that is rigid or soft is placed a distance $ks=3.0$ from the origin of the prolate spheroid and is

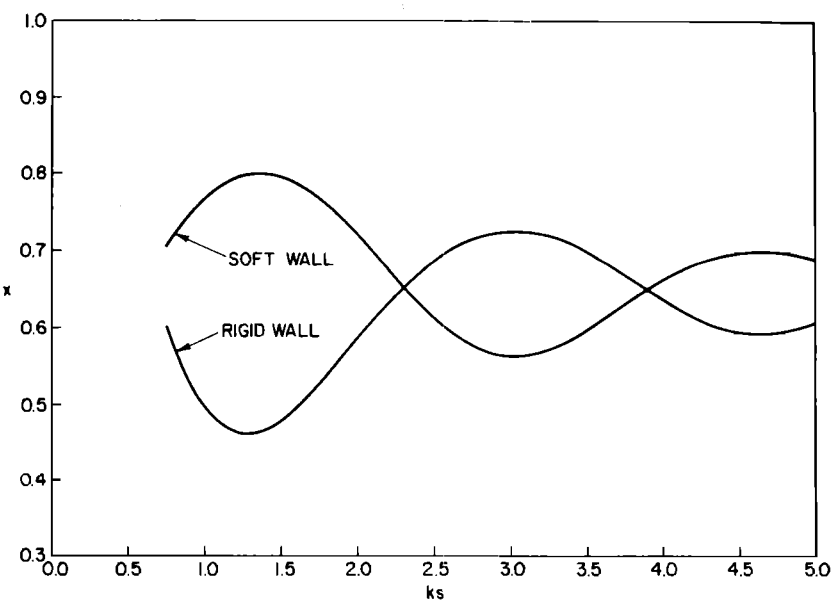

FIG. 9. The normalized radiation reactance as a function of the distance of separation ks for a disk vibrating in the presence of an infinite plane wall that is either rigid or soft.

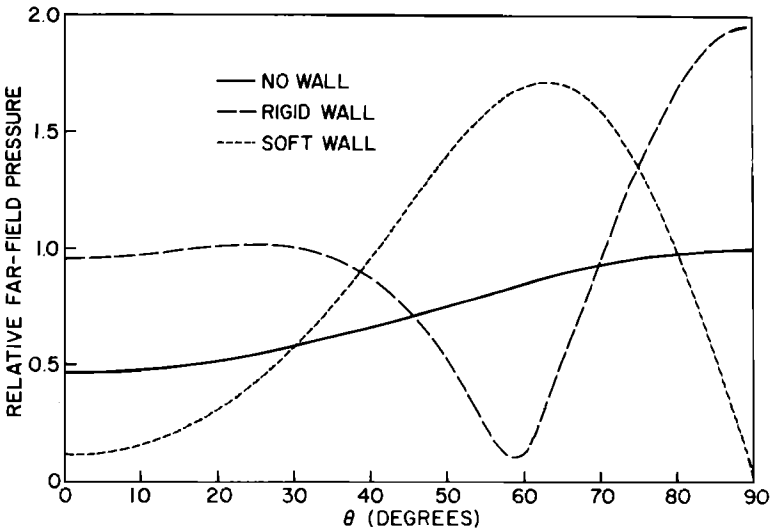

FIG. 10. The farfield pressure distribution for a prolate spheroid vibrating alone or in the presence of an infinite plane wall that is either rigid or soft.

oriented so that it is perpendicular to the major axis of the prolate spheroid. The farfield pressure distributions are normalized so that the value at $\theta=90°$ for the no-wall case is equal to unity. The wall has a significant effect on the farfield. Both the minimum for the rigid wall and the maximum for the soft wall which occur at about $\theta=60°$ are in qualitative agreement with the farfield pressure distribution calculated using monopole theory. Here the corresponding two-spheroid problem reduces to that of two point sources separated a distance $kr_{12}=6.0$. Note that the behavior of the curves around $\theta=90°$ (the farfield direction along the wall) is consistent with the boundary conditions imposed on the wall.

III. CONCLUSIONS

The acoustic radiation from two spheroids whose surface normal velocity distributions are specified was calculated using a Green's function technique. To simplify the analysis only axially symmetrical problems were considered. At the heart of the calculation is an addition theorem which expresses spheroidal wave functions in one coordinate system in terms of spheroidal wave functions in a second coordinate system with arbitrary relative position and orientation. This theory is applicable whether the two systems are both prolate, both oblate, or one prolate and one oblate. The generality of the addition theorem allows for the solution for any two-spheroid configuration. Of course, the Green's function must be written to include $m\neq 0$ terms when the problem does not have axial symmetry. The solution for more than two spheroids can be obtained by including in the Green's function an eigenfunction expansion about each spheroid.

[1] B. J. King, R. V. Baier, and S. Hanish, "A Fortran Computer Program for Calculating the Prolate Spheroidal Radial Functions of the First and Second Kind and Their First Derivatives," U. S. Naval Res. Lab. Rep. No. 7012 (1970).

[2] A. L. Van Buren, R. V. Baier, and S. Hanish, "A Fortran Computer Program for Calculating the Oblate Spheroidal Radial Functions of the First and Second Kind and Their First Derivatives," U. S. Naval Res. Lab. Rep. No. 6959 (1970).

[3] B. J. King and A. L. Van Buren, "A Fortran Computer Program for Calculating the Prolate and Oblate Angle Functions of the First Kind and Their First and Second Derivatives," U. S. Naval Res. Lab. Rep. No. 7161 (1970).

[4] T. Nimura and Y. Watanabe, "Sound Radiation from the Zonal Radiators," Tohoku Univ., Res. Inst. Sci. Rep., Ser. B **5**, 155–195 (1953).

[5] A. Silbiger, "Radiation from Circular Pistons of Elliptical Profile," J. Acoust. Soc. Amer. **33**, 1515–1522 (1961).

[6] G. Chertock, "Sound Radiation from Prolate Spheroids," J. Acoust. Soc. Amer. **33**, 871–876 (1961).

[7] S. Hanish, "The Numerical Computation of Radiation Impedance of Zonal Arrays on a Hard Prolate Spheroidal Baffle," U. S. Naval Res. Lab. Rep. No. 6108 (1964).

[8] A. L. Van Buren, "Acoustic Radiation Impedance of Caps and Rings on Prolate Spheroids," J. Acoust. Soc. Amer. **50**, 1343–1356 (1971).

[9] R. V. Baier, "Acoustic Radiation Impedance of Caps and Rings on Oblate Spheroidal Baffles," J. Acoust. Soc. Amer. **51** (May 1972).

[10] R. New, "Acoustic Radiation from Multiple Surfaces," Catholic Univ. Inst. Ocean Sci. Rep. No. 71-8 (1971).

[11] B. J. King and A. L. Van Buren, "A General Addition Theorem for Spheroidal Wave Functions," to be published in SIAM J. Math. Anal. **4**, No. 1.

[12] P. M. Morse and K. U. Ingard, *Theoretical Acoustics* (McGraw-Hill, New York, 1968).

[13] C. Flammer, *Spheroidal Wave Functions* (Stanford U. P., Stanford, Calif., 1957).

[14] S. Hanish, R. V. Baier, A. L. Van Buren, and B. J. King, "Tables of Radial Spheroidal Wave Functions, Vols. 1–3, Prolate, $m=0,1,2$," U. S. Naval Res. Lab. Rep. No. 7088-7090 (1970).

[15] S. Hanish, R. V. Baier, A. L. Van Buren, and B. J. King, "Tables of Radial Spheroidal Wave Functions, Vols. 4–6, Oblate, $m=0,1,2$," U. S. Naval Res. Lab. Rep. No. 7091–7093 (1970).